


Random telegraph noise in magnetically driven garnetsRobert Sponsel,¹ Aaron Hamann¹,* and E. Dan Dahlberg
University of Minnesota, Minneapolis, Minnesota 55455, USA (Received 15 July 2020; revised 5 January 2021; accepted 21 January 2021; published 8 April 2021)

Both the length scale and the magnetic field strength dependence of the magnetic noise in ac magnetically driven garnets were measured optically using the Faraday effect. At fields in a limited region, roughly twice the coercive field, the noise exhibits a Lorentzian power spectral density (PSD) consistent with random telegraph noise (RTN). The RTN onset as a function of applied field is rather abrupt and then decreases slowly with further increases in the applied field. The PSD of the noise in the lowest and highest magnetic field regimes is white background noise and is about two decades smaller than that of the RTN. In the field regime of the RTN, the PSD is Lorentzian at all measured length scales. As the measurement length scale increases past the order of a few microns, the low-frequency plateau of the Lorentzian PSD diminishes with increasing area measured as expected for a collection of uncorrelated RTN oscillators with similar characteristic frequencies.

DOI: [10.1103/PhysRevB.103.134411](https://doi.org/10.1103/PhysRevB.103.134411)**I. INTRODUCTION**

Significant studies of random telegraph noise (RTN) have occurred since its discovery in 1984 [1]. This phenomenon occurs across a large variety of systems with very different underlying physics. Despite the differences in the underlying physics, however, the basic model is that of a single entity switching between two energy states, separated by a barrier. Here, instead of a single entity, we investigate a system where the collective behavior of many entities, in this case domain wall pinning sites, results in RTN being observed in the overall structure or geometry of the magnetic domain structure of the 14 ferromagnetic garnets investigated. As expected, applying a small ac magnetic field perpendicular to the plane of a ferromagnetic garnet with perpendicular anisotropy results in sinusoidal oscillations of the widths of the domains. The portion of the domains parallel (antiparallel) to the field during an ac cycle increases (decreases) in size. As the magnitude of the ac field is increased to a field we will call H_{RTN} , low-frequency irreversible changes in the domain structure are observed. The power spectral density (PSD) of the fluctuations in the domain structure that start at H_{RTN} is Lorentzian, as expected for RTN. A Lorentzian PSD was observed for all sized areas from on the order of μm^2 to over 12 000 μm^2 . Although always a Lorentzian PSD, the magnitude of the noise decreased with increasing area.

As will be seen, it would appear that the two-well model commonly used to explain RTN provides an adequate description of this system. However, a strict interpretation of this model means that on length scales the order of a few microns, the magnetization fluctuates between two states that are separated by a single energy barrier. However, this cannot be the complete picture as it does not take the overall domain formation into account. In fact, the noise at relatively short length scales cannot be considered the result of a single fluctu-

ator but instead is due to the fluctuations in the overall domain structure of the sample, i.e., it is not a simple two-state system but a collective property related to the magnetic state of a specimen. In brief, the individual RTN oscillators collectively control the large-scale structures observed as RTN is observed throughout the samples. Thus the origin of the RTN is more complex. There have been recent observations [2,3] of similar behavior, although a detailed connection between those works and the present research is lacking.

What follows is a description of our experimental methods and then our experimental results. After that, we discuss how the low-frequency domain pattern fluctuations are explained by a collection of pinning sites acting as independent two-well RTN oscillators randomly trapping and releasing domains. Although the two-well oscillator model explains the data, there are significant differences between the current system and that model.

II. EXPERIMENTAL DETAILS

The 14 ferromagnetic garnet samples investigated were $\sim 10 \mu\text{m}$ thick and had various compositions of $(\text{Bi,Tm,Gd})_3(\text{Ga,Fe})_5\text{O}_{12}$ on a $\text{Gd}_3\text{Ga}_5\text{O}_{12}$ substrate; the samples were provided by either Allied Signal Corporation or manufactured by TEL-Atomic, Inc. [4]. Magneto-optical imaging (MOI), which utilizes the Faraday effect and polarizers, was used to image the domains. In general MOI has been applied to a variety of physical problems [5,6]. Studies somewhat related to our work is the observation of Barkhausen noise in films measured with magneto-optic techniques [7].

In zero applied magnetic field, the domain pattern in the samples falls into two groups, which we refer to as stripe and serpentine domains, as shown in Fig. 1. Ten of the samples had stripe domains, with domain widths varying from 10 to 25 μm . The other four had serpentine domains with an average width of approximately 8 μm .

The samples were placed in a short solenoid with a diameter of 5 mm. An ac current was used to create a sinusoidal

*Present address: University of Chicago Chicago, Illinois 60637, USA.

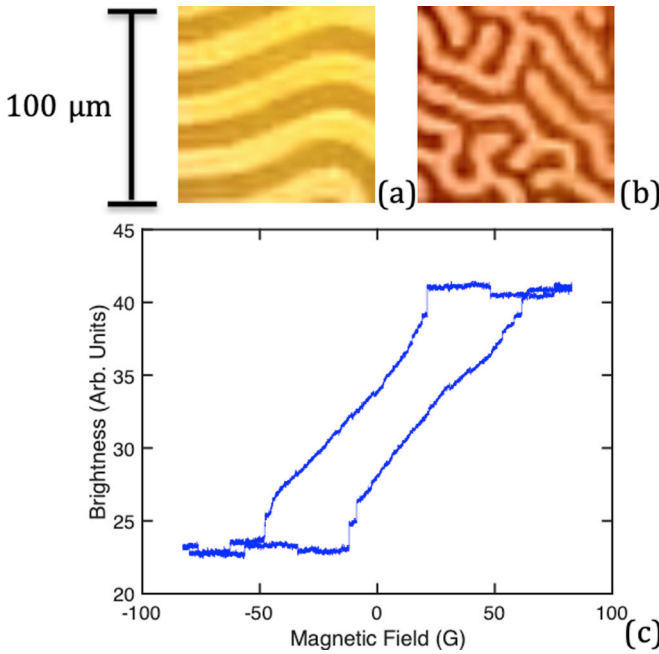


FIG. 1. Magneto-optical images showing (a) stripe or (b) serpentine domains in different sample types. Opposite direction domains appear as either bright or dark areas. A single scan hysteresis loop is shown in (c). In this single scan, Barkhausen jumps in the magnetization are observed.

oscillating magnetic field at frequencies from 1 to 450 Hz and peak magnetic fields up to 118 G for all the frequencies investigated. The results were similar for all frequencies, and the results presented here are those for data taken with a drive frequency of 250 Hz. At each end of the solenoid is a linear polarizer; one of the polarizers (the analyzer) could be rotated to any desired angle.

The coils and polarizers with the sample in place were mounted in a microscope with 20× amplification, and a camera was mounted to the microscope to record 1200 fps videos of the domains. The linearity of the camera sensor was tested via rotation of the analyzer to confirm that the measured signal was proportional to the cosine squared of the analyzer angle. For each sample, the analyzer angle was chosen to maximize contrast between domains.

The data consisted of video recordings of about 2 s in duration (2048 frames) for each ac magnetic field. In general, the PSDs at a given magnetic field are the average of 20 individual PSDs for the same field and at the same position on the sample.

For analysis of the data, each frame of a video was converted into a JPEG and imported into ImageJ [8], and the brightness (a scale of the signal between 0 and 256 from ImageJ) of each pixel (approximately a square of 2.5 μm on a side except where noted otherwise) in a video frame was measured. This produced a time record of the brightness for each pixel that corresponds to the magnetization of that region as a function of time. Then, a randomly selected area was chosen, and the brightness of these pixels was averaged into a single time record. This was then normalized for the average brightness for the entire video. For the area sampled

in a given PSD, the sizes reported are the length of a side of the square region. The PSD, $S_V(f)$, of each sized square was then determined by the equation

$$S_V(f) = \frac{|\hat{F}(f)|^2}{B_{\text{avg}}}, \quad (1)$$

where f is the frequency, $\hat{F}(f)$ is the Fourier transform of the time record, and B_{avg} is the total brightness of the area measured averaged over all frames.

III. RESULTS AND ANALYSIS

The primary result of this investigation is that the PSDs of all 14 samples investigated exhibited Lorentzian spectra as expected for RTN for fields greater than a critical ac field, with the ac field peak magnitude or maximum that was generally about twice the coercive field. For fields below the critical field, H_{RTN} , and for the largest magnetic fields, the PSDs exhibited white noise that we attribute to the measurement system. For the field region where the Lorentzian PSDs are observed, the larger the area investigated, the smaller is the noise.

PSDs for samples in zero field as well as for other nonmagnetic materials were measured. The zero-field PSDs show a relatively flat white noise floor at the same magnitude as those taken at low fields under similar circumstances. Comparing to magnitudes of PSDs with nonmagnetic materials is more difficult. Even when videos are normalized for brightness, the magnitude of the entire PSD can shift with changes in lighting or sample transparency. Nonmagnetic materials did produce a similar shaped white noise floor with a magnitude about an order of magnitude from the typical garnet samples. Also, for this reason, all of the data in the paper are from a single trial of videos taken under the same lighting conditions.

In what follows, we illustrate our results using data taken on a sample exhibiting straight domains with about a 13 μm domain width; these data are representative of the data taken on all the samples, including the serpentine domain samples. Examples of the noise at different magnetic fields for two different areas are shown in Fig. 2. The ac magnetic field drive frequency is clearly seen at 250 Hz; the value of the PSD at the drive frequency provides a useful metric to compare the noise between different ac fields and areas as confirmed by the linearity of the PSD at the drive frequency versus ac field strength (plot not shown). The data in Figs. 2(c) and 2(d) can be described with a Lorentzian PSD, $S_V(f)$, given by

$$S_V(f) = V_0^2 \frac{f_0}{1 + f^2/f_0^2}, \quad (2)$$

where V_0 is a measure of the noise magnitude, f is frequency, and f_0 is the average switching frequency. The average switching frequency is easily seen in the low-frequency segment of the PSDs; they are the frequencies where the PSD has a knee or flattens with decreasing frequency. Although easily seen in the data, the numeric values of all the attempt frequencies discussed here were determined by fitting the data to the Lorentzian PSD in Eq. (2). In general, when measured at 20 different areas on a given sample at the same ac field,

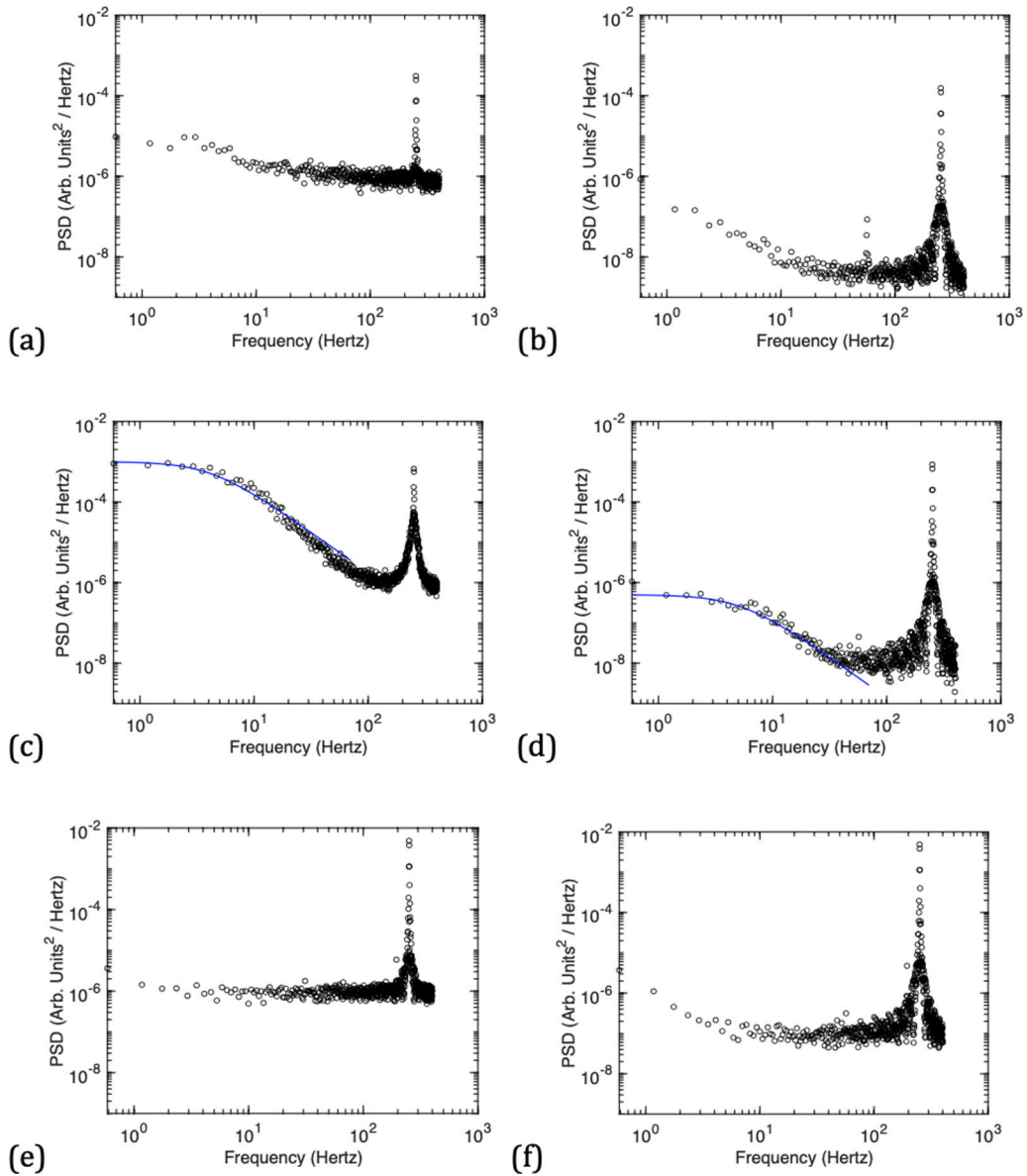


FIG. 2. The PSD for two different areas, a $6 \mu\text{m}^2$ square in the left column and a $12\,660 \mu\text{m}^2$ square in the right, at different fields of 14, 30, and 113 G from top to bottom. Both (a) and (b) were taken for fields less than H_{RTN} , (c) and (d) were taken at a field strength where the RTN noise is a maximum, and the bottom set (e) and (f) are for a field larger than the field range where RTN noise is observed. The solid lines (blue) in (c) and (d) are fitted to a Lorentzian, which was used to determine the knee frequency. Note that for (a), (b), (e), and (f), the noise is mostly white at frequencies less than the driving frequency of 250 Hz. These graphs are all from the same trial, with the same measurement location, same light intensity, and the same polarizer angle.

the knee frequencies, f_0 , were found to be within 25% of each other.

As the example in Fig. 3(a) shows, at applied fields less than H_{RTN} , the low-frequency noise at 3 Hz is white and has a magnitude independent of the applied field magnitude; this white noise is the background noise of the experimental system. As the field is increased to H_{RTN} (~ 26 G for this sample, approximately twice the coercive field), the low-frequency components of the PSD, those that would occur in the plateau of the PSD for RTN, abruptly increase by two orders of magnitude. As the field increases past the saturation field (~ 45 G for this sample), the Lorentzian spectrum diminishes and the

PSD effectively returns to the background white noise, as seen in the high field regime in Fig. 3(a).

In the field regime where the Lorentzian noise spectrum was present, the fitted values of the attempt frequency were found to be a function of the applied field, increasing exponentially with increasing field, as shown in Fig. 3(b). To understand the field dependence of the knee frequency, we start by noting that RTN is commonly modeled using a two-state energy system with the two states separated by an energy barrier. The system randomly switches from one minimum to the other with the aid of thermal fluctuations to transition over the barrier. The average switching frequency, the knee

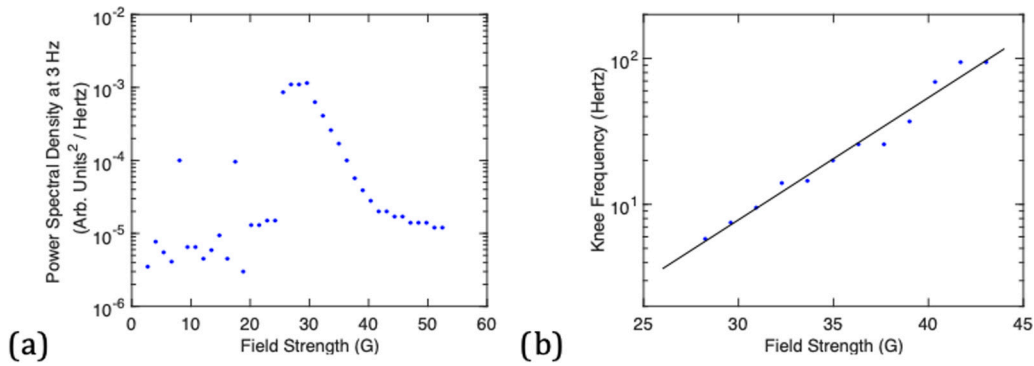


FIG. 3. (a) A semilog plot of the PSD magnitude at 3 Hz as a function of ac field strength. The peak of the magnitude of the noise happens at about 30 G, twice the coercive field. The log of the knee frequency as a function of ac field strength is shown in (b). The line in (b) is a fit to the Eq. (4) Arrhenius law. The scatter at low fields is due to random changes in the domain structure happening at a frequency smaller than the reciprocal of the measurement time.

frequency, f_0 , is given by the Arrhenius law [9],

$$f_0 = f_A e^{-U/k_B T}, \quad (3)$$

where f_A is the Arrhenius attempt frequency, k_B is Boltzmann's constant, T is the temperature, and U is the energy barrier.

For our case, the energy in the Boltzmann term of the Arrhenius law must include the effect of the applied field on the energy barrier for the escape from a given minimum. Including a Zeeman energy in the Arrhenius law, we obtain

$$f_0 = f_A e^{-\frac{U - |\mathbf{M} \cdot \mathbf{H}|}{k_B T}}, \quad (4)$$

where \mathbf{M} is the magnetization, \mathbf{H} is the applied field, and U is the zero magnetic field energy value for the barrier height. Note that in the current work, an ac magnetic field is applied and therefore the Zeeman energy term oscillates at the ac field frequency. Since the transition rate has an exponential dependence on the total energy barrier, a transition is most likely to occur when the field is close to or at its maximum value. For this reason, all magnetic field values are reported as the peak magnetic field value.

The exponential dependence of the Arrhenius attempt frequency on energy, including the Zeeman energy, results in the linear dependence of the log of the knee frequency, f_0 , versus H , as seen in Fig. 3(b). The three field regimes of the data in Fig. 3(a) are consistent with the above analysis. First, when the field is low, the energy barrier is much larger than $k_B T$ and there are no irreversible changes in the domain pattern. In other words, the increasing and decreasing size of the parallel and antiparallel magnetizations is reversible on the time scales we measure determined by the length of the time record. Next, as the magnitude of the ac field is increased, the energy barrier is lowered and the thermal fluctuations increase the occurrence of transitions resulting in RTN noise, as evidenced by the transition to RTN starting at approximately 26 G in Fig. 3(a). The third regime occurs for even larger applied fields that reduce the energy barriers to zero or very small, and therefore the magnitude of the RTN noise diminishes. This is seen at fields above about 45 G, where the noise begins to become indistinguishable from the white noise floor.

We will now discuss the results related to the measurement area. We will focus on those ac magnetic fields at about 30 G that produced the maximum RTN noise; again 3 Hz was chosen as a measurement of the Lorentzian spectrum in the low-frequency plateau region below the knee frequency. In Figs. 4(a) and 4(b) we plot the 3 Hz noise versus the area of the measurement with the light intensity normalized by the area measured. For all the data used in making this figure, we found the PSDs to be Lorentzian with attempt or knee frequencies that were identical within experimental error. First, we point out that the very noticeable oscillations for larger areas in Fig. 4(a) are attributed to an artifact of the length scales corresponding to an even number of domain widths producing a minimal average brightness. Although the measurement area is not exactly centered on an even number of domains, this would still cause a minimum in the magnitude of the noise.

An important feature of the data in Fig. 4(b) is that the noise decreases by about 2 decades as the area increases by 2 decades, suggesting that the noise is inversely proportional to the area analyzed; this is consistent with the straight line in Fig. 4(a) that has a slope of -1 .

Again, as in the field dependence of the energy barrier, we consider a two-state RTN oscillator. However, in this case it is not a single oscillator but a distribution of oscillators with similar knee frequencies. The inverse relation between the 1 Hz data and the area is consistent with a density of uncorrelated RTN oscillators with similar attempt frequencies (if there were a wide range spectrum of attempt frequencies, we would expect the noise to be more like $1/f$ as opposed to RTN) [10]. Measuring the time records over a distribution of uncorrelated oscillators produces a Lorentzian PSD with a smaller magnitude than any of the PSDs of the single oscillators. In particular, N identical oscillators will produce a PSD with magnitude $1/N$ compared to the PSD of an individual oscillator. Assuming that oscillators are roughly uniformly distributed across a sample, this would mean that the magnitude of noise measured should be inversely proportional to the area measured. Note that the fact the noise remains Lorentzian with roughly a constant knee frequency further confirms our previous comment that the knee frequencies measured at the smallest areas across a sample are similar. In general, there is

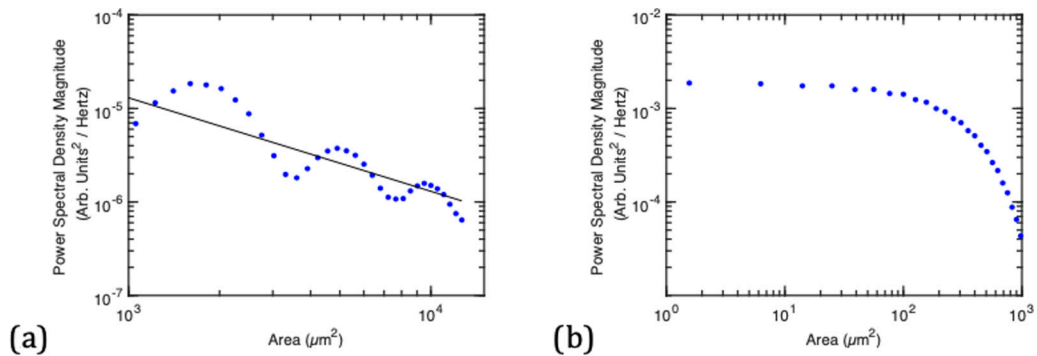


FIG. 4. Log-log plot showing the PSD at 3 Hz. As the area of measurement increases, the noise strength decreases. The black line is a guide to the eye with a slope of -1 . As mentioned in the text, the oscillation pattern is attributed to an artifact related to the domain period; it is independent of the specific analysis areas. Part (b) is from a measurement where the area measured was reduced by a factor of 3, and it indicates that at short length scales the noise magnitude becomes independent of area.

a lack of evidence from over 8000 videos that changing the location of measurement changes the knee frequency.

Figure 4(b) shows that at small areas, smaller than $50 \mu\text{m}^2$, the increase in noise with decreasing area trend terminates. This means that for this area and smaller, we are observing a single RTN oscillator. This indicates a density on the order of one RTN oscillator per $50 \mu\text{m}^2$, i.e., roughly 1000 RTN oscillators are in the maximum analysis area.

IV. DISCUSSION AND CONCLUSIONS

At first glance, the two-well model commonly used to explain RTN provides an adequate description of our system. A rigorous interpretation of this model would be that on length scales the order of a few microns, the magnetization fluctuates between two states that are separated by a single energy barrier. However, this cannot be the complete picture as it does not take the overall domain formation into account. In fact, the noise at relatively short length scales cannot be considered the result of a single fluctuator but instead is due to the fluctuations in the large-scale domain structure, i.e., it is not a simple two-state system but a collective property resulting in the domain pattern. Continuing with this, the basic Arrhenius model assumes switching between two states of an oscillator, but in our case it is unlikely that a given domain wall pinning site is involved in all RTN cycles, therefore the RTN we observe is global and not local. This global view is further complicated by the observation that as the sampling area is increased, the noise decreases. Again, this is as if one is measuring a collection of uncorrelated RTN oscillators with similar knee frequencies with a density of about one per $50 \mu\text{m}^2$ and not collective behavior.

Given that the domain structure changes occur on length scales much larger than the average separation of pinning sites, and that the onset of the noise occurs at magnetic fields on the order of the coercive field, we can describe our results with the following conceptual model. Consider a lattice of pinning sites to be responsible for the domain structure in zero applied magnetic field. For a given domain structure, some of the pinning sites are occupied by domain walls and some are not, with the specific occupation giving rise to the overall domain structure. As the ac magnetic field is increased,

the domain walls will move to accommodate the respective growing and shrinking of the domains, but the approximate shape of the domain structure remains the same. After the maximum field and the oscillating magnetic field again approaches zero field, most frequently the domain walls repin to these or spatially close to these pinning sites, and no change in the domain pattern is observed at the zero magnetic field point. Infrequently, however, a significant part of a domain wall shifts and the resulting domain pattern is altered. It is the infrequent nature of the process that leads to the observed RTN. One feature we find that may be important in this process is domains that have dead ends, i.e., they do not extend to the sample edges and they remain more or less stationary during the ac cycles, thus they may be key in the domain formation process see Fig. 1(b) for many examples of a dead end. Of course the above process is determined by the relevant energies. The obvious energy is that of the domain pinning sites, but what must also be included is an energy associated with the shape of the domain walls in the overall macroscopic structure, and this greatly complicates the development of an analytical model.

However, while there is no analytical model for the behavior of the domains, similar phenomena have been seen where small-scale dynamics gives rise to emergent structure or behavior on a larger scale [2,3]. The dynamics in our system between pinning sites and the overall domain structure also appears to display this multiscale behavior.

Although not shown here, we also calculated autocorrelations in the brightness as a function of distance for the individual still frames of the videos. As expected, they show an oscillating pattern similar to that of the oscillation artifact in Fig. 4(a), with an oscillation that has a period of two domain widths. Overall we find, as expected, that the autocorrelation increases with decreasing length scale from $20 \mu\text{m}^2$ to the shortest length of $1.3 \mu\text{m}^2$. Although this latter feature is anticipated, it is important as it confirms our interpretation that the plateauing of the noise in Fig. 4(a) for areas on the order of $100 \mu\text{m}^2$ can be interpreted as individual pinning centers. In other words, it rules out the plateau being an artifact of the spatial domain structure affecting the dynamical structure.

In conclusion, we find in the 14 garnet samples when driven by ac magnetic fields a distribution of random telegraph

noise oscillators pinning the domain walls. Surprisingly, the RTN oscillators in the samples appear to have approximately equal switching times and thus equal energy barriers. They are fairly uniformly distributed with a density of about one per $50 \mu\text{m}^2$. The decrease of the RTN with increasing measurement area indicates that the oscillators are uncorrelated. Lastly, as expected, the magnitude of the ac field lowers the energy barrier in a manner consistent with a simple interpretation of RTN.

ACKNOWLEDGMENTS

The authors thank Devlin Gualtieri (Allied Signal Corporation, Morristown, NJ) for many of the samples used in this investigation, and Michael Weissman for an interesting conversation. We also thank Maarten Rutgers and Jason Cleveland for preliminary studies of the noise in magnetic field driven garnets. This work was supported primarily by NSF Grant No. DMR 1609782.

-
- [1] K. S. Ralls, W. J. Skocpol, L. D. Jackel, R. E. Howard, L. A. Fetter, R. W. Epworth, and D. M. Tennant, Discrete Resistance Switching in Submicrometer Silicon Inversion Layers: Individual Interface Traps and ($1/f$?) Noise, *Phys. Rev. Lett.* **52**, 228 (1984).
 - [2] J. O'Byrne and J. Tailleur, Lamellar to Micellar Phases and Beyond: When Tactic Active Systems Admit Free Energy Functionals, *Phys. Rev. Lett.* **125**, 208003 (2020).
 - [3] J. D. Schieber, and M. Hütter, Multiscale Modeling Beyond Equilibrium, *Phys. Today* **73**, 36 (2020).
 - [4] Magnetic bubble apparatus, TEL-Atomic Incorporated, Jackson, MI, TEL-300.
 - [5] Y. L. Iunin, Y. P. Kabanov, V. I. Nikitento, X. M. Cheng, D. Clarke, O. A. Tretiakov, O. Tchernyshyov, A. J. Shapiro, R. D. Shull, and C. L. Chien, Asymmetric Domain Nucleation and Unusual Magnetization Reversal in Ultrathin Co Films with Perpendicular Anisotropy, *Phys. Rev. Lett.* **98**, 117204 (2007).
 - [6] Y. Deng, Y. Cheng, L. Xuan, and Z. Zeng, Principles of magneto-optic imaging and its applications, in *Integrated Imaging and Vision Techniques for Industrial Inspection: Advances in Computer Vision and Pattern Recognition*, edited by Z. Liu, H. Ukida, P. Ramuhalli, and K. Niel (Springer, London, 2015).
 - [7] D.-H. Kim, S.-B. Choe, and S.-C. Shin, Direct Observation of Barkhausen Avalanche in Co Thin Films, *Phys. Rev. Lett.* **90**, 087203 (2003).
 - [8] C. A. Schneider, W. S. Rasband, and K. W. Eliceiri, NIH Image to ImageJ: 25 years of image analysis, *Nat. Methods* **9**, 671 (2012).
 - [9] S. A. Arrhenius, Über die dissociationswärme und den einfluß der temperatur auf den dissociationsgrad der elektrolyte, *Z. Phys. Chem.* **4**, 96 (1889).
 - [10] B. N. Costanzi and E. Dan Dahlberg, Emergent $1/f$ Noise in Ensembles of Random Telegraph Noise Oscillators, *Phys. Rev. Lett.* **119**, 097201 (2017).